Experimental demonstration of a supergain three-dipole-end-fire-array

Alexandre Debard, Antonio Clemente, Lotfi Batel, Christophe Delaveaud

Experimental Demonstration of a Supergain Three-Dipole-End-Fire-Array

Alexandre Debard, Antonio Clemente, Lotfi Batel, Christophe Delaveaud
Univ. Grenoble-Alpes, CEA, Leti, F-38000, Grenoble, France
{antonio.clemente, christophe.delaveaud}@cea.fr

***Abstract*—This paper presents the experimental validation of a three-dipole array optimized for maximum gain. The complex excitation coefficients associated to the array are calculated using a synthesis procedure based on the array factor. A parasitic array architecture has been selected to implement the proposed antenna solution. The high gain reached (8.6 dBi for a *ka* of 1.4) shows the interest of the proposed optimization method. Furthermore, it was shown that this optimization method decreases the sensitivity to errors in the dipole excitation coefficients at the cost of a lower directivity compared to the superdirectivity.**

***Index Terms*— compact arrays, superdirectivity, supergain, small antennas, end-fire arrays.**

I. Introduction

Directive and compact antenna are a topic of interest in a plethora of emerging applications coming with the Internet of Things (IoT), wireless sensor networks, wireless power transfer or radiofrequency remote control. Research on superdirective end-fire arrays have been resumed since at least 2005 with the work from Altshuler et al. [1] demonstrating a practical superdirective array of two dipoles with a maximum directivity of 7 dBi. In [1], the complex excitation coefficients of each dipole was synthetized based on the Uzkov strategy [2]. In the last years, several other superdirective antenna demonstrations have been proposed in the literature considering a linear array of three and four elements [3]-[5]. While superdirectivity behavior has been demonstrated successfully, the achieved gain of these antennas was severely affected, especially increasing the number of elements and/or using a reduced inter-element distance.

In this paper, we propose to synthetize superdirective and high-efficiency end-fire arrays using a modified version of the method presented by Uzkov. This method is based on the survey of optimized linear arrays presented in [6], which includes a note on the possibility to maximize gain rather than directivity, considering the conducting losses of the radiating elements. To the best of the author's knowledge, excluding our preliminary work [7], this method has not be experimentally validated.

II. Optimization Method

A. Directivity Optimization

The far-field pattern of an array of P equally spaced radiating elements can be expressed by:

$$\vec{F}(\theta,\phi) = \sum_{p=1}^{P} a_p \overrightarrow{f_p}(\theta,\phi) e^{jk\vec{r}\cdot\vec{r}_p} \qquad (1)$$

where the a_p are the complex excitation coefficients, $\vec{r}$ is the unit vector in the far-field direction (θ,ϕ), and $k = \omega/c$ is the wavenumber. The terms $\overrightarrow{f_p}(\theta,\phi)$ are the element far-field patterns, phase referenced to their position defined by $\vec{r}_p$. Here, we assume that the terms $\overrightarrow{f_p}(\theta,\phi)$ in their environment do not change with the excitation coefficients. From [1] the directivity of the array in the (θ_0,ϕ_0) direction is expressed in the form:

$$D = \frac{\sum_{mp} a_m a_p^* \vec{f}_m \vec{f}_p^*}{\sum_{mp} a_m a_p^* R_{mp}} \qquad (2)$$

where $\vec{r}_0$ is the unit vector in the far-field direction (θ_0,ϕ_0). The term $\sum_{mp}$ denotes the double sum $\sum_{m=1}^{P}\sum_{p=1}^{P}$ and

$$R_{mp} = \frac{1}{4\pi}\int_0^{2\pi}\int_0^{\pi} \vec{f}_m \vec{f}_p^* e^{jk\vec{r}\cdot\vec{r}_m} e^{-jk\vec{r}\cdot\vec{r}_p} \sin\theta \, d\theta \, d\varphi \qquad (3)$$

The excitation coefficients a_{0p} maximizing the directivity expression in (2) are given by [2] or [6], as

$$\sum_{p=1}^{P} R_{mp}^* a_p = \vec{f}_m \cdot \alpha \cdot e^{-jk\vec{r}\cdot\vec{r}_m} \qquad (4)$$

with α an arbitrary constant.

B. Gain Optimization

Considering the loss resistances of each element of the array ($R_{loss,p}$) the gain (or IEEE gain) can be expressed as

$$G(\theta,\phi) = \frac{|\vec{F}(\theta,\phi)|^2}{\sum_{m=p}^{P}\sum_{l=1}^{P} a_m a_p^* R_{mp} + \sum_{p=1}^{P}|a_p|^2 R_{pp} r_{loss,p}} \qquad (5)$$

where the terms $r_{loss,p} = R_{loss,p}/R_{pp}$ are the normalized loss resistances [6]. Eq. (4) can thus be modified to maximize the gain by replacing the diagonal coefficients R_{pp} by $(1 + r_{loss,p})R_{pp}$, as

$$\sum_{p=1}^{P} R_{mp}^*(1 + \delta_{mp} r_{loss,p}) a_p = \vec{f}_m e^{-jk\vec{r}\cdot\vec{r}_m} \qquad (6)$$

with $\delta_{mp} = 0$ if $m \neq p$ and $\delta_{pp} = 1$.

The example of the directivity and gain optimizations of a three-infinitesimal-dipole array is shown in Fig. 1, where the peak directivities and gains are plotted as a function of inter-element spacing d. The results are displayed for both directivity and gain optimizations, considering a normalized loss resistance of 1% (efficiency of the elements equal to 99%). The complex coefficient a_p associated to the array elements to maximize the directivity and the gain are

synthetized using (4) and (6), respectively. It is interesting to observe that for a reduced inter-element spacing, the optimization of the gain gives higher levels than the gain obtained in the case of the directivity optimization.

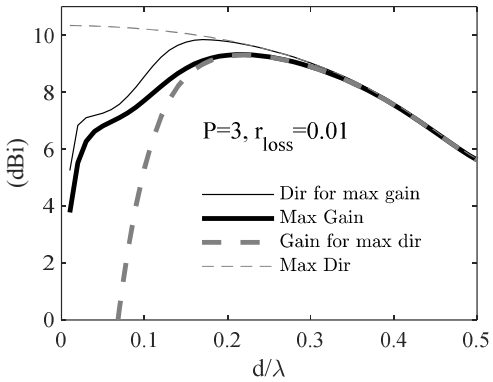

Fig. 1. Directivity and gain as a function of the inter-element spacing of a three-infinitesimal-dipole array. 'Max Gain' or 'Max Dir' indicate that the gain or the directivity is optimized, respectively. 'Gain for max dir' is the gain reached when the directivity is optimized. Contrariwise, 'Dir for max gain' indicates the achieved directivity when the gain is optimized. The loss resistance considered is $r_{loss} = 0.01$.

III. Parasitic Array Design and Simulation Results

This section details the design of the antenna array prototype including its feeding balun. The proposed antenna prototype is an array of three printed bent dipoles as it is shown in Fig. 2. The dipoles are spaced of a distance equal to 0.12λ, which is equal to 4.2 cm at the chosen working frequency of 850 MHz. The dielectric substrate on which the copper dipoles are printed on is the Rogers 4003 (permittivity of 3.38, a tan δ of 0.0027, and a thickness of 1.524 mm). The total length of the dipoles is 0.44λ, while their height (h in Fig. 2) is equal to $\frac{2\times0.44}{3}\lambda$. Only the dipole located at the center is fed, while the other ones are loaded with complex impedance loads. These loads are calculated from the complex excitation coefficients synthetized with (6) by following the procedure detailed in the Section III.C.

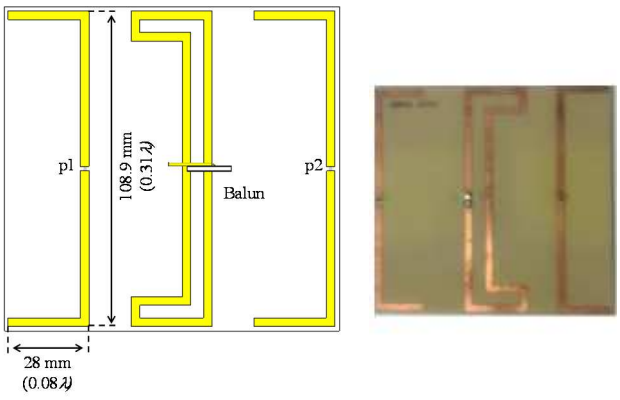

(a) (b)

Fig. 2. Three-dipole array prototype. (a) Schematic view and (b) photograph of the realized prototype.

A. Design of the Fed Dipole Element

The fed dipole is folded. This is done to increase its radiation resistance as it was shown that the radiation resistance R_{rad}^{folded} of a folded dipole is equal to

$$R_{rad}^{folded} = N_f^2 R_{rad} \qquad (7)$$

where N_f is the number of folding arms ($N_f = 2$) and R_{rad} *is* the radiation resistance of the dipole without folding [8]. The interest of this technique for this type of array was presented in [9], as the radiation resistance of the array decreases with the spacing between dipoles and the increase in directivity.

B. Balun Design and Characterization

A specific printed balun has been designed separately from the antenna array to feed the balanced dipole located at center of the array. This balun is illustrated in Fig. 3 and its measured scattering parameters in magnitude and phase are respectively plotted over the frequency band 750-950 MHz in Fig. 4 and Fig. 5.

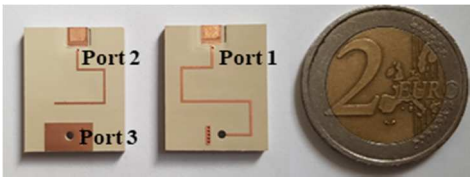

Fig. 3. Photograph of the prototyped balun.

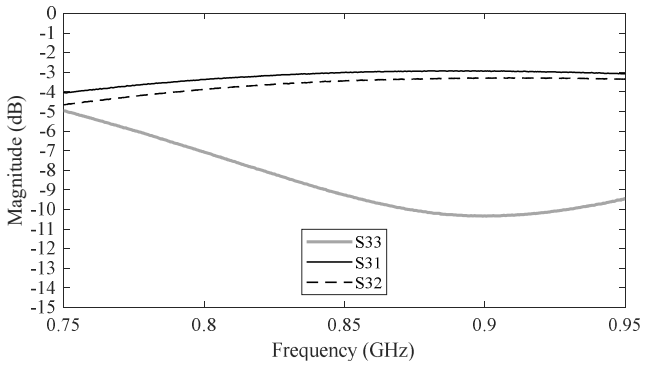

Fig. 4. Measured magnitude of the S-parameters of the balun, as a function of frequency.

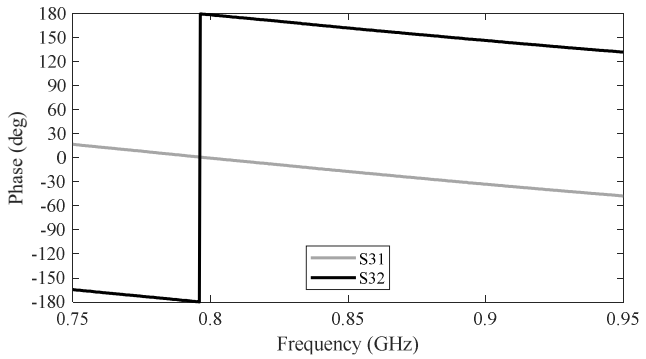

Fig. 5. Measured phase in degrees of the S-parameters of the balun, as a function of frequency.

As shown in Fig.4, reflection coefficient at the unbalanced input of the balun (Port 3) achieves -6 dB bandwidth from 775 to 1060 MHz, with an impedance matching less than -10 dB around 850 MHz. S21 and S31 parameters correspond to the transmission coefficient between the unbalanced input (Port 3) and the two balanced outputs (Port 1 and Port 2). Fig.4 shows a low insertion loss around 0.4 dB at 850 MHz. Moreover, Fig. 5 shows a phase shift of 180° between the two outputs of the balun at 850 MHz. Those two parameters lead to validate the performance of the compact fabricated balun at the frequency of interest.

C. *Simulations and parasitic element load calculation*

The fed antenna was simulated (CST MWS) with its balun but without the rest of the array to estimate its radiation efficiency. The calculated radiation efficiency is $\eta_1 = 96\%$. The radiation efficiency of the other dipoles without balun was rounded up by the simulation software to $\eta_2 = \eta_3 = 100\%$. The average radiation of the dipoles is then equal to

$$\eta = \frac{0.96+1+1}{3} \qquad (8)$$

$$\eta = 99\%$$

The loss resistance can be calculated from the radiation efficiency as

$$r_{loss} = \frac{1-\eta}{\eta} \qquad (9)$$

Hence, for $\eta = 99\%$, $r_{loss} = 1\%$, which corresponds to the loss value used to plot the curves displayed in Fig. 1. With an inter-element spacing of $0.12\ \lambda$, the expected directivity and gain for an array of three infinitesimal dipole are 9.2 dBi and 8.2 dBi, respectively.

The accurate optimization of the array could be done thanks to the full-wave simulation, which could compute the radiated field of each element of the array, considering the presence of the other elements. This provides the value of $\vec{f_p} e^{-jk\vec{r}.\vec{r_p}}$ for each dipole ($p = 1$ to 3), allowing the calculation of the R_{mp} and thus the optimized excitation coefficients a_p from equation (6). Note that the normalized loss resistances $r_{loss,p}$ were also calculated again through the full-wave simulation, this time considering the presence of all the dipole in the array.

The impedance values $Z_{L,p}$ of the load for the parasitic elements of the array were then extracted from the excitation coefficients a_p and the mutual impedances of the array Z_{mp}, as

$$Z_{L,p} = \frac{\sum_{m=1}^{P} Z_{mp} a_m}{a_p} \qquad (10)$$

The mutual impedances Z_{mp} were also calculated by electromagnetic simulations. In order to maximize gain, the real part of these load impedance was neglected, so the parasitic loads consisted of a capacitor of 22 pF for the director dipole and a capacitor of 33 pF for the reflector dipole. The simulated 3D gain pattern of the array is displayed in Fig. 6, showing a maximum gain of 7.85 dBi, with a frequency shift of the maximum gain to 830 MHz instead of 850 MHz. The summary of the results is shown in Table I.

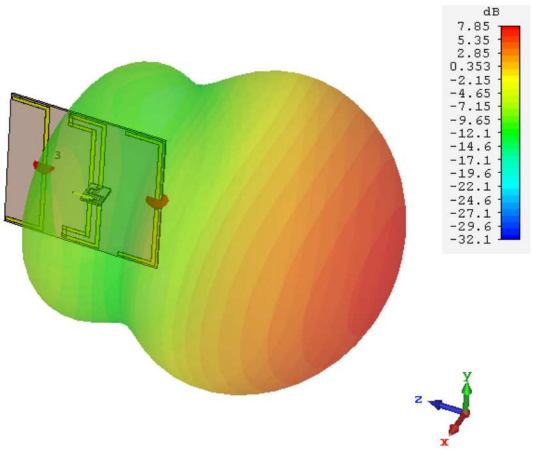

Fig. 6. Simulated 3D radiation gain pattern of the array optimized for maximum gain. The scale represents the IEEE gain (in dBi).

TABLE I. MAXIMUM DIRECTIVITY, MAXIMUM GAIN AND FREQUENCY OF MAXIMUM GAIN FOR A THREE-DIPOLE ARRAY ACCORDING TO THEORY, FULL-WAVE SIMULATION AND MEASUREMENTS. THE PARASITIC LOADS USED IN THE MEASUREMENTS AND THE SIMULATION ARE ALSO INDICATED.

	Theory	**Simulation**	**Measurements**
Frequency (MHz)	850	830	840
Directivity (dBi)	9.2	8.9	9.1
Gain (dBi)	8.2	7.8	8.6
$C_2(pF)$		22.0	22.0
$C_3(pF)$		33.0	33.0

IV. MEASUREMENT RESULTS

The fabricated prototype was measured in the CEA-Leti anechoic chamber that can be seen in Fig. 7 showing the measurement set-up. The antenna under test is in the foreground and the measurement horn antenna can be seen in the background. The gain radiation pattern was measured in the horizontal $\phi = 0°$ and vertical $\phi = 90°$ planes. The radiated power needed to derive the directivity was extracted by integrating both plane and interpolating the rest of the radiation pattern. The measured directivity and (IEEE) gain as a function of frequency are shown in Fig. 8 and compared to the simulated results. The measured and simulated directivity radiation patterns compute on the $\phi = 0°$ and $\phi = 90°$ cut-planes are also plotted in Fig. 9.

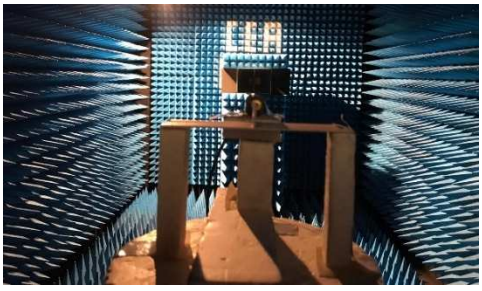

Fig. 7. Measurement set-up in anechoic chamber.

The measured peak directivity equal to 9.1 dBi and gain of 8.6 dBi have been achieved at 840 MHz. These should be compared to the values of 8.9 dBi and 7.8 dBi computed in full wave simulation at 830 MHz. The 10 MHz of frequency shift is probably due to the sensitivity of the simulation and to the tolerances of the capacitive loads used in the prototype.

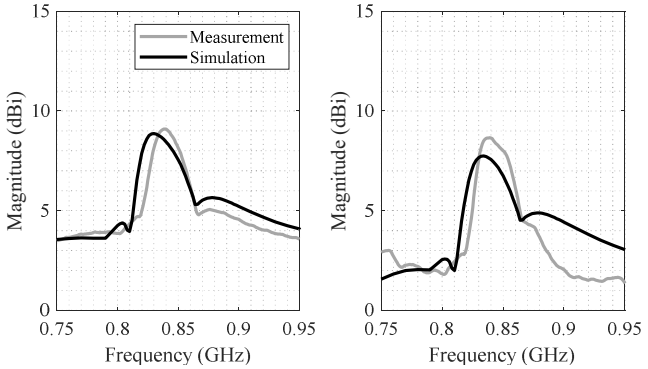

Fig. 8. Measured and simulated peak directivity (left) and gain (right) of the proposed and-fire array as a function of frequency.

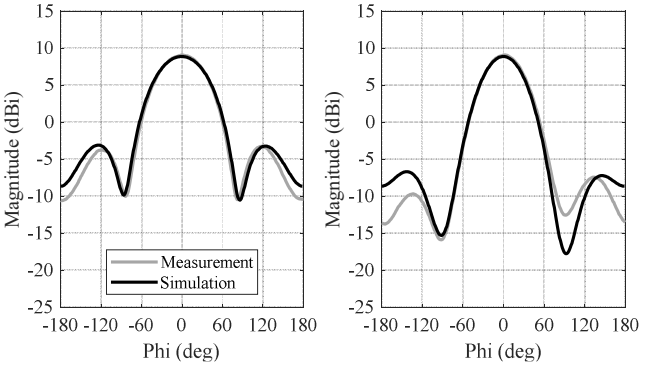

Fig. 9. Measured and simulated directivity radiation patterns of the proposed end-fire array computed on the cut-planes $\phi = 0°$ (left) and $\phi = 90°$ (right). Measurement and simulation frequencies are equal to 840 and 830 MHz, respectively. They are selected in agreement with the peak values.

V. Conclusion

In this paper the experimental demonstration of an end-fire supergain linear array with a gain of 8.6 dBi has been presented. A three-element array based on parasitic technology has been designed and optimized. The complex parasitic loads associated to the array elements have been synthetized considering a specific procedure based on the array factor.

Acknowledgment

The authors would like to thank Dr. HDR P. Pouliguen and Dr. P. Potier for their useful suggestions and comments on the work presented in this manuscript. This work is partially supported by the DGA (Direction générale de l'armement).

References

[1] E. E. Altshuler, T. H. O'Donnell, A. D. Yaghjian, and S. R. Best, "A monopole superdirective array," *IEEE Trans. Antennas Propag.*, vol. 53, no. 8, pp. 2653–2661, Aug. 2005.

[2] A. I. Uzkov, "An approach to the problem of optimum directive antennae design," *Comptes Rendus de l'Académie de Sciences de l'URSS*, vol. 53, no. 1, pp. 35-38, 1946.

[3] O. S. Kim, S. Pivnenko, and O. Breinbjerg, "Superdirective magnetic dipole array as a first-order probe for spherical near-field antenna measurements," *IEEE Trans. Antennas Propag.*, vol. 60, no. 10, pp. 4670–4676, Oct. 2012.

[4] A. Clemente, M. Pigeon, L. Rudant, and C. Delaveaud, "Design of a super directive four-element compact antenna array using spherical wave expansion," *IEEE Trans. Antennas Propag.*, vol. 63, no. 11, pp. 4715–4722, Nov. 2015.

[5] M. Hammoud, A. Haskou, A. Sharaiha, and S. Collardey, "Small end-fire superdirective folded meandered monopole antenna array," *Microw. Opt. Technol. Lett.*, vol. 58, no. 9, pp. 2122–2124, Sep. 2016.

[6] Collin, Robert E., et Francis J. Zucker. Antenna Theory [by] Robert E. Collin [and] Francis J. Zucker., 1969.

[7] A. Debard, A. Clemente, C. Delaveaud, C. Djoma, P. Potier, and P. Pouliguen, "Limitations and optimization of supergain end-fire arrays", in *Proc. Eu. Conf Antennas Propag.* (*EuCAP 2019*), Kracov, Poland, 2019.

[8] A. R. Clark and A. P. C. Fourie, "Mutual impedance and the folded dipole", in *Proc. Second International Conference on Computation in Electromagnetics*, Apr. 1994.

[9] S. R. Best, "Improving the performance properties of a dipole element closely spaced to a PEC ground plane," *IEEE Antennas Wireless Propag. Lett.*, vol. 3, pp. 359–363, 2004.